Chiral and achiral phosphine derivatives of alkylidyne tricobalt carbonyl clusters as catalyst precursors for (asymmetric) inter- and intramolecular Pauson–Khand reactions†

Viktor Moberg,[a] M. Abdul Mottalib,[a] Désirée Sauer,[a] Yulia Poplavskaya,[a] Donald C. Craig,[b] Stephen B. Colbran,[b] Antony J. Deeming[c] and Ebbe Nordlander*[a]

Received 20th November 2007, Accepted 31st January 2008
First published as an Advance Article on the web 13th March 2008
DOI: 10.1039/b717698h

Phosphine derivatives of alkylidyne tricobalt carbonyl clusters have been tested as catalysts/catalyst precursors in intermolecular and (asymmetric) intramolecular Pauson–Khand reactions. A number of new phosphine derivatives of the tricobalt alkylidyne clusters $[Co_3(\mu_3\text{-}CR)(CO)_9]$ (R = H, CO_2Et) were prepared and characterised. The clusters $[Co_3(\mu_3\text{-}CR)(CO)_{9-x}(PR'_3)_x]$ (PR'_3 = achiral or chiral monodentate phosphine, x = 1–3) and $[Co_3(\mu_3\text{-}CR)(CO)_7(P\text{–}P)]$ (P–P = chiral diphosphine; 1,1′- and 1,2-structural isomers) were assayed as catalysts for intermolecular and (asymmetric) intramolecular Pauson–Khand reactions. The phosphine-substituted tricobalt clusters proved to be viable catalysts/catalyst precursors that gave moderate to very good product yields (up to ~90%), but the enantiomeric excesses were too low for the clusters to be of practical use in the asymmetric reactions.

Introduction

The Pauson–Khand reaction[1,2] may be viewed as a [2 + 2 + 1] cycloaddition reaction between an alkyne, an alkene, and carbon monoxide leading to the formation of a cyclopentenone (Scheme 1), and inter- and intramolecular[3] Pauson–Khand cyclizations are widely employed in synthetic organic chemistry. The cyclization reaction is effected by polynuclear metal complexes that may be used as either stoichiometric reagents or catalysts. In the original Pauson–Khand reaction,[1] the alkyne was coordinated to $[Co_2(CO)_8]$ forming $[Co_2(CO)_6(alkyne)]$ which was heated in the presence of a suitable alkene. It has been found that the cyclization reaction can be accelerated by the addition of promoters, *e.g.* tertiary amine oxides which effect oxidative decarbonylation[1,4] or hard Lewis bases (alcohols, amines) which promote CO dissociation.[1,5] Other metal-based reagents, *e.g.* titanocenes,[6] have been used for cyclocarbonylation of enynes and new synthetic methods for cyclopentenone synthesis have also been developed.[7]

Catalytic Pauson–Khand cyclization reactions were first described by Pauson and co-workers.[8] Sugihara *et al.*[2,9] have shown that alkylidyne tricobalt carbonyl clusters are efficient catalysts/catalyst precursors for Pauson–Khand reactions, and other transition metal clusters, *e.g.* $[Ru_3(CO)_{12}]$,[10] have also been used to catalyse this cycloaddition reaction. While cyclizations leading to cyclopentenones that are substituted in positions 4 and 5 of the cyclopentenone invariably lead to the *exo* compound, cyclopentenones that are substituted only in position 4 give rise to enantiomers. Enantioselective and diastereoselective catalytic Pauson–Khand reactions have been developed by adding auxiliary chiral ligands, *e.g.* BINAP, to $[Co_2(CO)_8]$.[11,12] Considering the excellent catalytic properties that have been reported for $[Co_3(\mu_3\text{-}CR)(CO)_9]$ (R = H, CO_2Et),[2,9] we have prepared chiral derivatives of alkylidyne tricobalt carbonyl clusters *via* coordination of chiral phosphines to the cluster backbone in order to investigate the catalytic properties of the new clusters in enantioselective Pauson–Khand reactions. Here we report the preparation of a number of achiral and chiral phosphine-substituted alkylidyne tricobalt carbonyl clusters, *viz.* $[Co_3(\mu_3\text{-}CR)(CO)_{9-x}(PR'_3)_x]$ (x = 1–3: R = CO_2Et, PR'_3 = PEt_3; R = H, PR'_3 = PMe_2Ph), $[Co_3(\mu_3\text{-}CH)(CO)_8\{(S)\text{-NMDPP}\}]$, $[\{Co_3(\mu_3\text{-}CH)(CO)_8\}_2(\mu\text{-P–P})]$ (P–P = dppe, dppm) and $[Co_3(\mu_3\text{-}CH)(CO)_7(P\text{–}P)]$ [P–P = (*R*,*R*)-DIPAMP, (*S*,*S*)-CHIRAPHOS, (*R*)-BINAP, (*R*)-(*S*)-Josiphos3, (*R*,*R*)-Me-DUPHOS, (*R*)-PROPHOS, (*R*,*R*)-NORPHOS)],‡ and their abilities to catalyze (enantioselective) Pauson–Khand cyclizations.

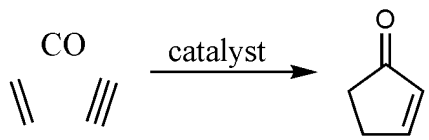

Scheme 1 General reaction scheme for the intermolecular catalytic Pauson–Khand reaction.

[a]*Inorganic Chemistry Research Group, Chemical Physics, Center for Chemistry and Chemical Engineering, Lund University, Box 124, SE-221 00, Lund, Sweden. E-mail: Ebbe.Nordlander@chemphys.lu.se; Fax: (+46) 46 222 44 39*
[b]*School of Chemistry, University of New South Wales, Sydney, NSW, 2052, Australia*
[c]*Department of Chemistry, University College London, 20 Gordon Street, London, UK WC1H OAJ*

† Electronic supplementary information (ESI) available: Figure S1. Two views (with 30% thermal ellipsoids) of the 'bent' carbonyl ligand in the crystal structure of $[Co_3(\mu_3\text{-}CH)(CO)_7(\mu\text{-}1,2\text{-DIPAMP})]$ (**12**). CCDC reference numbers 668301–668304. For crystallographic data in CIF or other electronic format see DOI: 10.1039/b717698h

‡ These ligands are hereafter referred to without chirality notation, *i.e.* DIPAMP = (*R*,*R*)-DIPAMP *etc.*

Results and discussion

New phosphine-substituted alkylidyne tricobalt carbonyl clusters

A number of mono- and bidentate phosphine derivatives of $[Co_3(\mu_3\text{-}CR)(CO)_9]$ (R = H, CO_2Et) of the general formulae $[Co_3(\mu_3\text{-}CR)(CO)_{9-x}(PR'_3)_x]$ (x = 1–3) and $[Co_3(\mu_3\text{-}CR')(CO)_7(P\text{–}P)]$ (P–P = bidentate phosphine) were synthesized according to established synthetic procedures (see below and Experimental section). In addition, new clusters with the less common structures that are depicted in Fig. 1 could also be isolated from these syntheses. The chiral ligands that have been used in this investigation are depicted in Fig. 2.

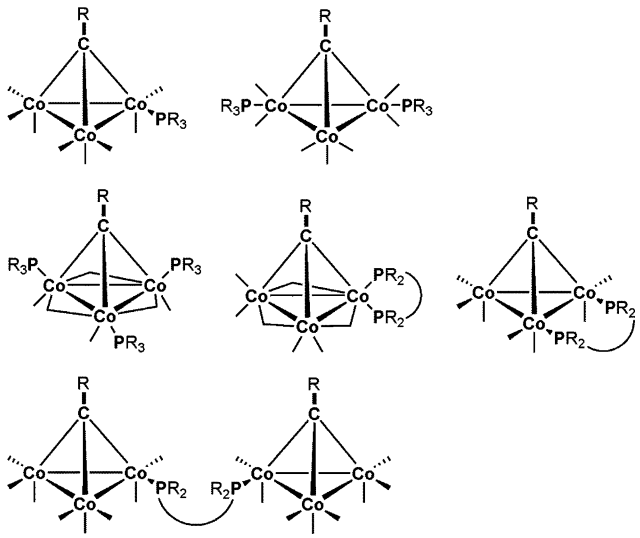

Fig. 1 Schematic structures of the phosphine coordination modes in the new cobalt clusters that have been prepared in this study.

Derivatives of monodentate phosphine ligands. The parent clusters $[Co_3(\mu_3\text{-}CR)(CO)_9]$ (R = CO_2Et, H) were reacted with either a stoichiometric amount (1 eq.) or an excess of phosphine ligand, PEt_3 or PMe_2Ph, in dichloromethane at room temperature. When one equivalent of the ligand was used, the mono- and di-phosphine-substituted clusters were obtained in moderate yields {**1**: $[Co_3(\mu_3\text{-}CO_2Et)(CO)_8(PEt_3)]$, 50%; **2**: $[Co_3(\mu_3\text{-}CH)(CO)_8(PMe_2Ph)]$, 46%; **3**: $[Co_3(\mu_3\text{-}CH)(CO)_7(PEt_3)_2]$, 11%; **4**: $[Co_3(\mu_3\text{-}CH)(CO)_7(PMe_2Ph)_2]$, 17%}. When an excess of the relevant phosphine was used, the corresponding trisubstituted clusters $[Co_3(\mu_3\text{-}CR)_6(PR'_3)_3]$ were the exclusive products and were isolated in moderate to relatively good yields [R = H: PR'_3 = PEt_3 (**5**) (50%), PMe_2Ph (**6**) (75%)]. Clusters **1–6** were identified on the basis of NMR and IR spectroscopy, mass spectrometry and elemental analyses, which were consistent with the proposed molecular formulae. The IR spectra of clusters **1**, **5** and **6** are typical of phosphine-substituted alkylidyne tricobalt carbonyl complexes.[13,14] The IR spectra of **2**, **3** and **4** in cyclohexane solution exhibit weak bands in the region 1880–1824 cm^{-1} that indicate that these clusters contain bridging carbonyl ligands but no such bands could be detected in the solid state (KBr pellet) IR spectrum of **2**.

The chiral monodentate ligand NMDPP (Fig. 2) was reacted with $[Co_3(\mu_3\text{-}CH)(CO)_9]$ at elevated temperature for 4 h. Only one product was isolated and identified as the mono-substituted cluster

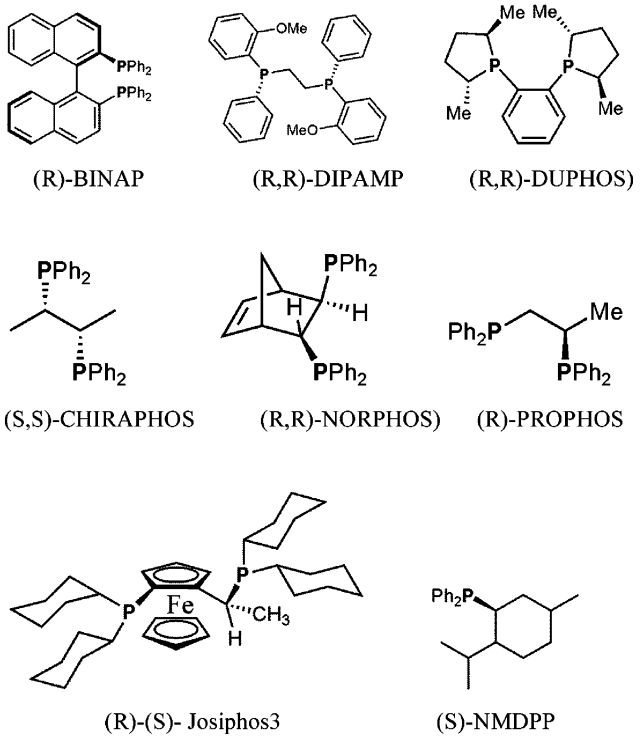

Fig. 2 Structures of the chiral ligands used in this investigation.

$[Co_3(\mu_3\text{-}CH)(CO)_8(NMDPP)]$ (**7**) in 51% yield. The spectroscopic data from IR, ^1H and ^{31}P NMR measurements, the mass spectrum and the microanalysis are in full agreement with the suggested formula. In addition to the typical IR bands found in monosubstituted alkylidyne tricobalt clusters, the spectrum reveals a signal at 1858 cm^{-1} similar to that found in clusters **2** and **4**.

Derivatives of bidentate phosphine ligands. The parent cluster $[Co_3(\mu_3\text{-}CH)(CO)_9]$ was reacted with a stoichiometric amount (1 eq.) of a diphosphine ligand P–P (P–P = dppe, dppm) in toluene at room temperature. Both bridged dimers, $[\{Co_3(\mu_3\text{-}CH)(CO)_8\}_2(\mu\text{-}P\text{–}P)]$, and disubstituted monomeric clusters, $[Co_3(\mu_3\text{-}CH)(CO)_7(P\text{–}P)]$, were obtained. The isolated yields of $[\{Co_3(\mu_3\text{-}CH)(CO)_8\}_2(\mu\text{-}P\text{–}P)]$ were low to moderate (P–P = dppe (**8**), 25%; dppm (**9**), 4%) while the disubstituted $[Co_3(\mu_3\text{-}CH)(CO)_7(P\text{–}P)]$ clusters were formed in relatively good yields (P–P = dppe (**10**), 50%; dppm (**11**), 67%). The chiral bidentate phosphine DIPAMP (see Fig. 2) was reacted with a stoichiometric amount of the parent cluster, which led to the formation of $[Co_3(\mu_3\text{-}CH)(CO)_7(DIPAMP)]$ (**12**) in 79% yield. The clusters **8–12** were characterised by NMR and IR spectroscopy, mass spectrometry and elemental analysis, all of which were consistent with the proposed molecular formulae.

The chiral diphosphines CHIRAPHOS, BINAP, NORPHOS, Me-DUPHOS and PROPHOS (see Fig. 2) were reacted with a stoichiometric equivalent of $[Co_3(\mu_3\text{-}CH)(CO)_9]$ in refluxing (CHIRAPHOS, BINAP) or warm (40 °C) hexane, which gave $[Co_3(\mu_3\text{-}CH)(CO)_7(P\text{–}P)]$ in good yields (P–P = BINAP (**13**), 51%; CHIRAPHOS (**14**), 98%; NORPHOS (**15**), 55%; PROPHOS (**16**), 59%; Me-DUPHOS (**17**), 70%). Clusters **13–17** were analysed and identified on the basis of NMR and IR spectroscopy and mass spectrometry, which were in agreement with the proposed molecular formulae. Cluster **17** shows distinct absorption bands at

1863 and 1819 cm^{-1}, indicating the presence of bridging carbonyls, which was verified by the molecular structure obtained from X-ray diffraction analysis (*vide infra*).

Reaction of the chiral diphosphine Josiphos3 (Fig. 2) with $[Co_3(\mu_3\text{-}CH)(CO)_9]$ in refluxing dichloromethane gave $[Co_3(\mu_3\text{-}CH)(CO)_7$(Josiphos3)] (**18**) in 83% yield. Cluster **18** was characterised by NMR and IR spectroscopy and mass spectrometry. The FAB mass spectrum confirmed the proposed molecular formula. However, ^1H and ^{31}P NMR as well as IR spectra indicate the presence of isomers in solution. The peak areas in the ^1H NMR spectra show some inconsistency. While the peaks for all protons on the ligand integrate correctly, the peak for the μ_3-methylidyne proton only measures 1/3 of the expected peak area. In the ^{31}P NMR, a set of six resonances are observed at δ 32.7 (s), 37.2 (s) 39.9 (s), 54.2 (s), 61.2 (s) and 69.8 (s). A variable temperature ^{31}P NMR experiment (Fig. 3) revealed that the intensities of the peaks at δ 37.2 and 39.9 decreased as the temperature was raised, until at 333 K (60 °C) they almost disappeared. In contrast, the two peaks at δ 54.2 and 69.8 increased significantly when the sample was heated (Fig. 3). The observed isomerisation process was reversible; once the temperature was decreased to ambient temperature (298 K), the intensities of peaks at δ 37.2 and 39.9 increased, while the peak intensities at δ 54.2 and 69.8 decreased. The intensities of the peaks at δ 32.7 and 61.2 were unaffected by the temperature. These results indicate that there are multiple isomers present in the solution of cluster **18**. The isomers may be configurational isomers that involve different bonding modes of the diphosphine and (or) carbonyl ligands. For example, $[Co_3(\mu\text{-}CR)(CO)_7$(P–P)] clusters have been shown to undergo reversible isomerisation reactions wherein the coordination mode of the diphosphine changes between chelating and bridging.[15] We postulate that such an equilibrium exists for **18**, with a chelating isomer, in which both phosphine moieties are coordinated in equatorial positions on the $Co_3(\mu_3\text{-}CR)$ framework, interconverting with the corresponding bridged dimer. As the two phosphine moieties of the Josiphos3 are inherently different, two ^{31}P resonances are observed for each isomer. The third isomer, which does not interconvert with the two other isomers, is proposed to contain the diphosphine in a chelating coordination mode, but with one phosphine moiety coordinating in the (unique) axial site of one cobalt atom and the second phosphine moiety coordinating in an equatorial site on the same cobalt. Bridging and chelating coordination modes for Josiphos3 at a tetrahedral cluster core have been detected for two isomers of $[H_4Ru_4(CO)_{10}$(Josiphos3)][16] but in this case no interconversion between the two isomers has been detected. The fluxionality/equilibrium that has been observed for **18** may be due to a poorer fit of the ligand in the bridging mode than in the tetraruthenium cluster – the Co–Co distance in **18** is approximately 0.5 Å shorter than in the tetraruthenium cluster and this may cause a strain in the seven-membered ring that is formed when the diphosphine bridges a metal–metal bond, thus enabling interconversion of the two isomers at relatively low energies. An alternative explanation is that the two interconverting isomers have the same (bridging) coordination mode of the diphosphine and the configurational isomerism consists of an interconversion of terminal and bridging carbonyl ligands, while the third, non-interconverting isomer contains the diphosphine ligand in a different (chelating) coordination mode. It may be expected that the energy barrier for such an isomerization reaction is relatively low. Finally, it is possible that two diastereomeric forms of **18** exist – the bridging coordination of a heterodidentate ligand to a metal triangle leads to the formation of enantiomers[17] which, in combination with the chirality of the enantiomerically pure phosphine ligand, leads to the formation of two diastereomers, one of which may be involved in configurational isomerism.

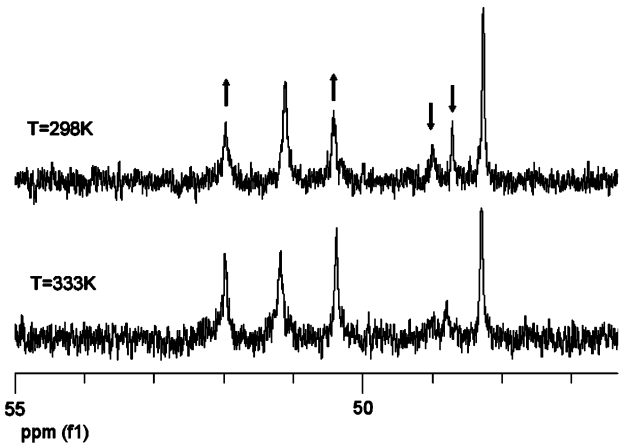

Fig. 3 ^{31}P NMR spectra of $[Co_3(\mu_3\text{-}CH)(CO)_7\{(R)\text{-}(S)$-Josiphos3}] (**18**) showing the increase/decrease of peak intensities upon heating of the sample.

X-Ray crystallography

$[Co_3(\mu_3\text{-}CH)(CO)_8(PMe_2Ph)]$ (2). The molecular structure of cluster **2** is shown in Fig. 4 and relevant bond lengths and angles are reported in Table 1. The three cobalt atoms form a triangle which is capped by the μ_3-CH moiety, and the dimethylphenyl phosphine ligand is equatorially coordinated to Co(3). The cobalt atoms complete their pseudo-octahedral coordination spheres with terminal carbonyl ligands. The Co–Co bonds are notably different in lengths, ranging from 2.4636(6) Å [Co(2)–Co(3)] to 2.4899(5) Å [Co(1)–Co(3)], and are similar to those found in the related cluster $[Co_3(\mu_3\text{-}CC(O)NHPr^i)(CO)_8(PPh_3)]$.[13] The average of the three Co–Co distances (2.4746 Å) is similar to those

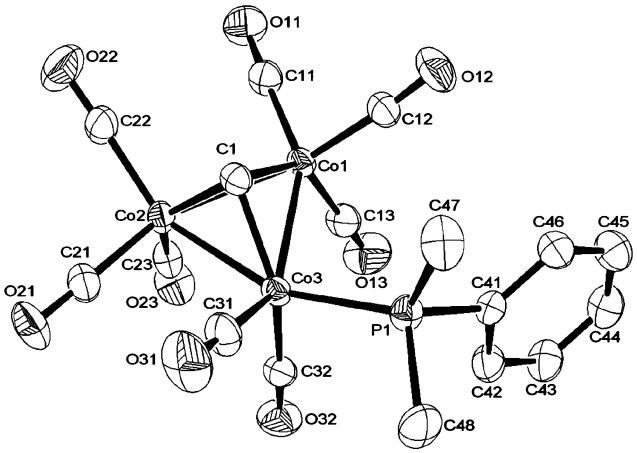

Fig. 4 An ORTEP drawing of the molecular structure of $[Co_3(\mu_3\text{-}CH)(CO)_8(PMe_2Ph)]$ (**2**) showing the atom numbering scheme. Thermal ellipsoids are drawn at the 30% probability level. For the sake of clarity, all hydrogen atoms have been omitted.

Table 1 Relevant bond lengths (Å) and angles (°) for clusters $[Co_3(\mu_3\text{-}CH)(CO)_8(PMe_2Ph)]$ (**2**), $[Co_3(\mu_3\text{-}CH)(CO)_6(PMe_2Ph)_3]$ (**6**), $[Co_3(\mu_3\text{-}CH)(CO)_7(\mu\text{-}1,2\text{-DIPAMP})]$ (**12**) and $[Co_3(\mu_3\text{-}CH)(CO)_7(1,1\text{-DUPHOS})]$ (**17**)

Cluster **2**			
Co(1)–Co(2)	2.4703(5)	Co(1)–Co(3)	2.4899(5)
Co(2)–Co(3)	2.4636(6)	Co(1)–C(1)	1.888(3)
Co(2)–C(1)	1.913(3)	Co(3)–C(1)	1.881(3)
Co(1)–C(11)	1.792(4)	Co(1)–C(12)	1.761(3)
Co(1)–C(13)	1.814(3)	Co(2)–C(21)	1.777(4)
Co(2)–C(22)	1.791(4)	Co(2)–C(23)	1.807(4)
Co(3)–C(31)	1.773(3)	Co(3)–C(32)	1.808(4)
Co(3)–P(1)	2.1981(9)	P(1)–C(41)	1.819(3)
P(1)–C(47)	1.810(4)	P(1)–C(48)	1.828(4)
P(1)–Co(3)–Co(1)	100.05(3)	C(31)–Co(3)–P(1)	91.56(12)
P(1)–Co(3)–Co(2)	158.70(3)	C(32)–Co(3)–P(1)	97.30(11)
C(1)–Co(3)–P(1)	112.40(10)		

Cluster **6**			
Co(1)–Co(2)	2.4445(9)	Co(1)–Co(3)	2.4436(9)
Co(2)–Co(3)	2.4377(9)	Co(1)–C(7)	1.889(5)
Co(2)–C(7)	1.888(5)	Co(3)–C(7)	1.895(5)
Co(1)–P(1)	2.1632(16)	Co(1)–C(1)	1.958(6)
Co(1)–C(3)	1.920(6)	Co(1)–C(4)	1.751(6)
Co(2)–P(2)	2.1660(17)	Co(2)–C(1)	1.936(6)
Co(2)–C(2)	1.973(5)	Co(2)–C(5)	1.754(6)
Co(3)–P(3)	2.1705(15)	Co(3)–C(2)	1.918(6)
Co(3)–C(3)	1.972(6)	Co(3)–C(6)	1.756(7)
Co(3)–Co(2)–Co(1)	60.07(3)	Co(3)–Co(1)–Co(2)	59.83(3)
Co(2)–Co(3)–Co(1)	60.11(3)	C(6)–Co(3)–P(3)	100.6(2)
P(3)–Co(3)–Co(2)	133.38(5)	C(7)–Co(3)–P(3)	97.31(16)
P(3)–Co(3)–Co(1)	128.08(5)	C(7)–Co(2)–P(2)	95.79(17)
C(5)–Co(2)–P(2)	102.0(2)	P(2)–Co(2)–Co(1)	130.85(5)
P(2)–Co(2)–Co(3)	128.66(5)	C(7)–Co(1)–P(1)	95.96(16)
C(4)–Co(1)–P(1)	101.5(2)	P(1)–Co(1)–Co(2)	128.28(6)
P(1)–Co(1)–Co(3)	131.57(5)		

Cluster **12**			
Co(1)–Co(2)	2.500(2)	Co(1)–Co(3)	2.444(2)
Co(1)–P(1)	2.171(3)	Co(1)–CC(1)	1.796(12)
Co(1)–CC(1)	1.758(12)	Co(1)–CH	1.839(10)
Co(2)–Co(3)	2.506(2)	Co(2)–P(2)	2.212(3)
Co(2)–CC(3)	1.792(12)	Co(2)–CC(4)	1.773(11)
Co(2)–CH	1.912(10)	Co(3)–CC(5)	1.764(16)
Co(3)–CC(6)	1.791(17)	Co(3)–CC(7)	1.572(12)
Co(3)–CH	1.935(11)	P(1)···P(2)	3.692
P(1)–Co(1)–CC(2)	93.7(4)	P(1)–Co(1)–CC(1)	101.4(3)
Co(1)–Co(2)–P(2)	103.24(8)	P(1)–Co(1)–CH	100.7(3)
P(2)–Co(2)–CC(3)	100.2(4)	Co(3)–Co(2)–P(2)	156.35(9)
P(2)–Co(2)–CH	107.2(3)	P(2)–Co(2)–CC(4)	94.2(4)
Co(3)–CC(7) OC(7)	140.7(18)		

Cluster **17**			
Co(1)–Co(2)	2.528(1)	Co(1)–Co(3)	2.501(1)
Co(1)–P(1)	2.218(1)	Co(1)–P(2)	2.171(1)
Co(1)–CC(1)	1.888(5)	Co(1)–CC(2)	1.832(6)
Co(1)–CH	1.889(5)	Co(2)–Co(3)	2.432(1)
Co(2)–CC(1)	2.054(5)	Co(2)–CC(3)	1.773(6)
Co(2)–CC(4)	1.785(6)	Co(2)–CC(7)	2.008(5)
Co(2)–CH	1.905(5)	Co(3)–CC2)	2.175(6)
Co(3)–CC(5)	1.769(6)	Co(3)–CC(6)	1.797(6)
Co(3)–CC(7)	1.902(6)	Co(3)–CH	1.905(4)
P(1)···P(2)	3.074		

Table 1 (*Contd.*)

Cluster **17**			
Co(3)–Co(1)–P(1)	130.58(4)	Co(2)–Co(1)–P(1)	132.95(5)
P(1)–Co(1)–P(2)	88.90(5)	P(1)–Co(1)–CH	178.4(2)
Co(3)–Co(1)–P(2)	136.18(4)	P(2)–Co(1)–CH	90.9(1)
Co(2)–Co(1)–P(2)	112.41(5)		

found in tricobalt alkylidyne nonacarbonyl clusters, *e.g.* $[Co_3(\mu_3\text{-}CMe)(CO)_9]$ ($Co\text{–}Co_{mean}$ = 2.467 Å),[18] $[Co_3(\mu_3\text{-}CPh)(CO)_9]$ ($Co\text{–}Co_{mean}$ = 2.467 Å),[19] $[Co_3(\mu_3\text{-}CC(O)Ph)(CO)_9]$ ($Co\text{–}Co_{mean}$ = 2.470 Å),[20] in numerous phosphine derivatives of the type $[Co_3(\mu_3\text{-}CR)(CO)_{9-x}(PR_3)_x]$[12,19–23] and $[Co_3(\mu_3\text{-}CR)(CO)_7(P\text{–}P)]$,[13,24] and also for Co–Co bonds found in various polynuclear cobalt complexes.[25] The PMe_2Ph ligand coordinates in an equatorial position relative to the Co triangle, *i.e. cis* to a metal–alkylidyne bond, as seen for other monosubstituted tricobalt alkylidyne clusters, *e.g.* $[Co_3(\mu_3\text{-}CC(O)NHPr^i)(CO)_8(PPh_3)]$[13] and $[Co_3(\mu_3\text{-}CMe)(CO)_7\{PPh_2(C_4H_3S)\}_2]$.[21] The Co–P bond length [2.1981(9) Å] is normal for a Co–PR_3 bond,[26] *e.g.* $[Co_3(\mu_3\text{-}CMe)(CO)_7\{PPh_2(C_4H_3S)\}_2]$ ($Co\text{–}P_{mean}$ = 2.212 Å), but significantly shorter than the Co–P distance found in $[Co_3(\mu_3\text{-}CC(O)NHPr^i)(CO)_8(PPh_3)]$ (2.2400 Å).[13] The average Co–C(1) distance (1.894 Å) does not show any significant deviation from other reported alkylidyne nonacarbonyl clusters and their phosphine derivatives.[13]

$[Co_3(\mu_3\text{-}CH)(CO)_6(PMe_2Ph)_3]$ (6). Fig. 5 presents a view of cluster **6** and relevant bond lengths and angles are summarised in Table 1. The three cobalt atoms in the cluster core form an almost equilateral triangle capped by the μ_3-methylidyne moiety. Each dimethylphenyl phosphine ligand is equatorially bound to one cobalt atom and is *cis* to an alkylidyne carbon–cobalt bond. Cluster **6** contains three terminal carbonyls and three edge-bridging carbonyls (μ-CO), which is consistent with the μ-CO stretches seen in its IR spectrum (*vide supra*). The μ-CO groups are located in equatorial positions with no deviation from the plane defined by the triangular cobalt cluster core.

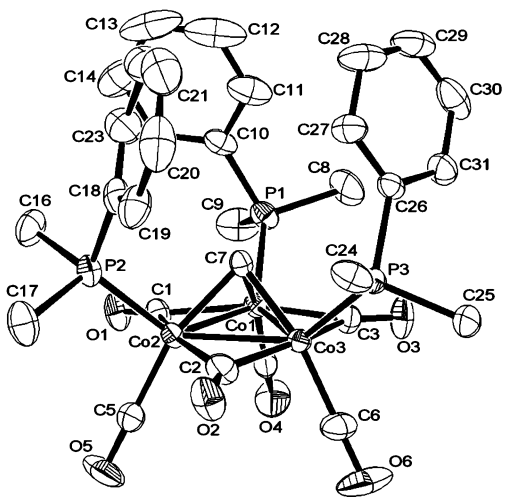

Fig. 5 An ORTEP drawing of the molecular structure of $[Co_3(\mu_3\text{-}CH)(CO)_6(PMe_2Ph)_3]$ (**6**) showing the atom numbering scheme. Thermal ellipsoids are drawn at the 30% probability level. For the sake of clarity, all hydrogen atoms have been omitted.

The cobalt carbon distances for the three μ-CO groups range from 1.918(6) Å [Co(3)–C(2)] to 1.973(5) Å [Co(2)–C(2)], with an average distance of 1.946 Å, and are somewhat longer than those observed in $[Co_3(\mu_3\text{-CPh})(CO)_7(1,1\text{-bpcd})]$ [bpcd = 4,5-bis(diphenylphosphino)-4-cyclopenten-1,3-dione] (1.92 Å).[27] The three Co–Co bond lengths exhibit a mean distance of 2.4419 Å, which is significantly shorter than that found in **2**. The three Co–P distances vary from 2.163(2) Å [Co(1)–P(1)] to 2.170(2) Å [Co(3)–P(3)], and $Co–P_{mean}$ (2.1665 Å) is slightly shorter than that found in cluster **2** [2.1981(9) Å]. All three phosphorus atoms in the coordinated ligands occupy axial positions, *cis* to the capping μ_3-methylidyne moiety. There is a pseudo-C_3 axis going through the alkylidyne C–H bond so that the phenyl moieties of the phosphines form a cage around the μ_3-methylidyne moiety (Fig. 6).

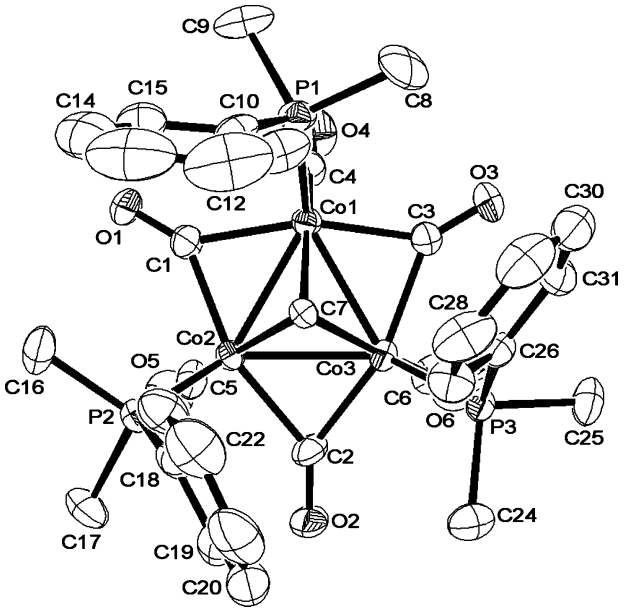

Fig. 6 An ORTEP drawing of the molecular structure of $[Co_3(\mu_3\text{-CH})(CO)_6(PMe_2Ph)_3]$ (**6**), giving a clear view of the pseudo-C_3 axis through the apical C–H bond.

$[Co_3(\mu_3\text{-CH})(CO)_7(\mu\text{-1,2-DIPAMP})]$ (12). The molecular structure of **12** is shown in Fig. 7 (bond lengths and angles are summarised in Table 1); it verifies the bridging coordination of the diphosphine ligand DIPAMP across the Co(1)–Co(2) bond. The Co–Co bond lengths in **12** are significantly different, ranging from 2.506(2) Å [Co(2)–Co(3)] to 2.444(2) Å [Co(1)–Co(3)] and show an average distance of 2.483 Å. All carbonyls are terminal and both phosphorus donors of the DIPAMP ligand are coordinated in equatorial positions. The axial carbonyl group of Co(3) deviates significantly from linearity, exhibiting a bond angle of 140.7(18)° [Co(3)–Cc(7)–Oc(7)] suggestive of sp^2 rather than sp hybridization for carbon Cc(7). Bent metal–carbonyl bonds occur rather frequently in transition metal carbonyl complexes. In this case, it may be assigned to weak hydrogen bonding present between the alkylidyne tricobalt carbonyl clusters in the crystal lattice, as described by Desiraju[28] and Braga *et al.*[29] The cobalt to alkylidyne carbon bond distances are notably different, 1.839(10) Å [Co(1)–CH], 1.912(10) Å [Co(2)–CH] and 1.935(11) Å [Co(3)–CH], *i.e.* the μ_3-capping methylidyne moiety

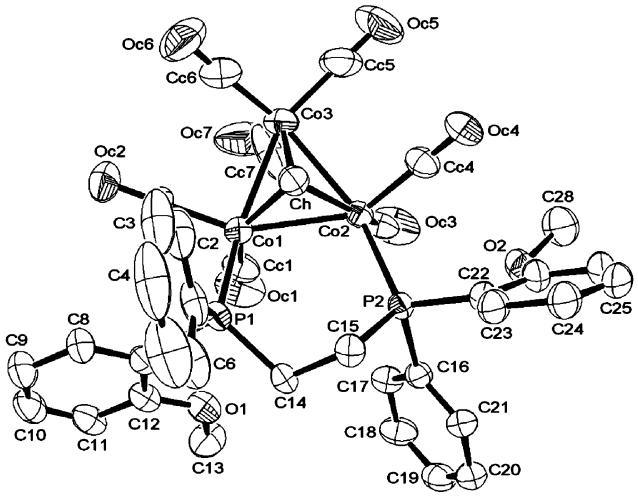

Fig. 7 An ORTEP drawing of the molecular structure of $[Co_3(\mu_3\text{-CH})(CO)_7(\mu\text{-1,2-DIPAMP})]$ (**12**) showing the atom numbering scheme. Thermal ellipsoids are drawn at the 30% probability level. For the sake of clarity, all hydrogen atoms have been omitted.

is leaning towards the two cobalt atoms bearing the phosphine ligand. This phenomenon has been observed previously and has been reported by Downard *et al.*[30] The apical carbon adopts a "semicapping orientation" with respect to the triangular array of cobalt atoms. It is suggested that the observed displacement is a result of the uneven increase of electron density on the CCo_3 core, as a consequence of the substitution of carbonyl ligands with (di)phosphines. The di-equatorial diphosphine ligand prevents the carbonyl ligands from adopting bridged coordination modes that would assist in the dissipation of electron density from the metals. An alternative, electron dispersion may occur through the interaction of appropriate p-orbitals on the capped carbon and the d-orbitals of Co(1) and Co(2).[30] The Co–P distances are somewhat different in length, 2.171(3) Å [Co(1)–P(1)] and 2.212(3) Å [Co(2)–P(2)]. The mean Co–P bond length in cluster **12** (2.192 Å) is similar to that found in **17** (2.194 Å, *vide infra*), and in range for what is acceptable for $Co–PR_3$ bonds.[26]

$[Co_3(\mu_3\text{-CH})(CO)_7(1,1\text{-Me-DUPHOS})]$ (17). The molecular structure of **17** is shown in Fig. 8 and relevant bond lengths and angles are summarised in Table 1. Cluster **17** contains a chelating DUPHOS ligand coordinated to Co(1), forming a five-membered ring. The two phosphine moieties of the ligand are located in axial positions, almost perpendicular to the Co_3-plane, as previously found in the cluster $[Co_3(\mu_3\text{-CPh})(CO)_7(1,1\text{-bpcd})]$.[27] The Co–Co bond lengths in the cluster, which range from 2.432(1) Å [Co(2)–Co(3)] to 2.528(1) Å [Co(1)–P(1)], differ significantly. The two metal–metal bonds involving Co(1) are long [Co(1)–Co(2) = 2.528(1) Å, Co(1)–Co(3) = 2.501(1) Å], while the Co(2)–Co(3) distance is approximately 0.08 Å shorter. The length of the two former bonds may be due to a buildup of electron density on Co(1) caused by the coordination of the diphosphine but the average length of the Co–Co bonds, 2.487 Å, is in the same range as other Co–Co single bonds found in related clusters.[13,24,27] As in the case of **6**, cluster **17** contains three bridging CO ligands, which is consistent with its IR spectrum. The cobalt–carbonyl carbon bond lengths exhibit a mean distance of 1.976 Å, similar to that found in **6** (1.946 Å). Two of the bridging carbonyl ligands in cluster **17**,

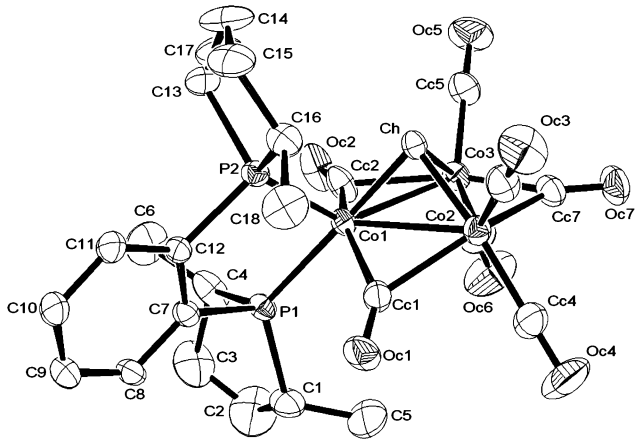

Fig. 8 An ORTEP drawing of the molecular structure of $[Co_3(\mu_3\text{-}CH)(CO)_7(1,1\text{-}DUPHOS)]$ (**17**) showing the atom numbering scheme. Thermal ellipsoids are drawn at the 30% probability level. For the sake of clarity, all hydrogen atoms have been omitted.

[Co(1)–Co(3) and Co(2)–Co(3)] coordinate in the same manner as seen in cluster **6**. The carbonyl bridging the Co(1)–C(2) edge is notably affected by the bulky phosphine ligand, being forced out of the triangular plane by 23.6°, in relative *trans* position to the capping μ_3-CH moiety.

The two P–Co vectors are slightly different, 2.218(1) Å [Co(1)–P(1)] and 2.171(1) Å [Co(2)–P(2)] ($Co–P_{mean}$ = 2.194 Å). The observed [P(1)–Co(1)–P(2)] bond angle, 88.90(5)°, is similar to the P–Co–P angle found in the related structure $[Co_3(\mu_3\text{-}CPh)(CO)_7(1,1\text{-}bpcd)]$ (89.2°)[27] but notably larger than that observed in the ruthenium cluster $[H_4Ru_4(CO)_{10}(1,1\text{-}DUPHOS)]$ (83.7° or 85.3°).[31] The two phosphorus atoms in the DUPHOS ligand are separated by two relatively rigid sp^2-hybridized carbons, thus favouring a relatively close approach of the phosphorus atoms [P(1)–P(2) = 3.074 Å] with their lone pairs directed so that a chelating coordination mode of the ligand is favoured. On the other hand, the phosphine moieties in DIPAMP are bridged by two sp^3-hybridized carbon atoms that make the backbone less rigid/more flexible and permit the ligand to bridge a metal–metal bond as in **12** (*vide supra*).

Catalysis experiments

The catalytic properties of the phosphine-substituted alkylidyne tricobalt carbonyl clusters in inter- and intramolecular Pauson–Khand reactions were investigated. The initial studies were carried out on clusters with achiral phosphines, in order to establish that Pauson–Khand cyclizations could indeed be achieved with phosphine-substituted clusters. These studies were followed by attempts to achieve enantioselective intramolecular Pauson–Khand reactions. In addition, one attempt to hydrogenate 2-methyl-2-butenoic (tiglic) acid using $[Co_3(\mu_3\text{-}CH)(CO)_7(PMe_2Ph)_2]$ (**4**) as a catalyst was made, using conditions similar to those reported for H_4Ru_4 clusters;[31,32] however, no hydrogenation of the substrate could be detected.

Intermolecular Pauson–Khand reaction. Clusters **2**, **4**, **6**, **16** and **17** were successfully used as catalyst precursors in the intermolecular cyclization of norbornene and phenyl acetylene in the presence of carbon monoxide (Scheme 2). The reaction was carried out in toluene at 120 °C under a pressure carbon monoxide of 10 bar with tricobalt cluster and substrates. No additives were used. The isolated yield of the cyclopentenone product, 4-phenyltricyclo[5.2.1.$0^{2,6}$]dec-4-en-3-one (**19**) (Scheme 2) varies notably for the different catalysts, ranging from moderate to good (see Table 2). The disubstituted cluster **4** gave the highest isolated yield (90%) of **19**. It was somewhat surprising to find that the monosubstituted cluster **2** gave notably lower yield of **19** (75%) than **4**, as multiple substitution of the metal carbonyl cluster is expected to make the cluster less prone to further CO loss/substitution. The results from the diphosphine-derivatised clusters **16** and **17**, 65 and 70% respectively, are notably lower than that of **4** but somewhat higher than for **2**. In the case of **16** and **17**, no cluster was recovered after a complete catalytic experiment, while experiments performed with **2**, **4** and **6** gave a red, air-stable crystalline compound which thus far has eluded identification. The above-mentioned observations suggest that the cobalt–alkylidyne clusters are indeed precursors to active catalysts.

Table 2 Results from catalytic intermolecular Pauson–Khand synthesis

		Yield[b] (%)	
Entry	Catalyst[a]	**19**	Triphenylbenzene
1	**2**	75	13
2	**4**	90	6
3	**6**	45	15
4	**16**	65	—
5	**17**	70	—

[a] *Reaction conditions*: *n*(substrate)/*n*(catalyst) = 50, *p*(CO) = 10 bar, *T* = 120 °C, solvent = toluene, duration = 10 h. [b] Isolated yields after prep. TLC (hexane–ethyl acetate 4 : 1 v/v) (see Experimental section for further details).

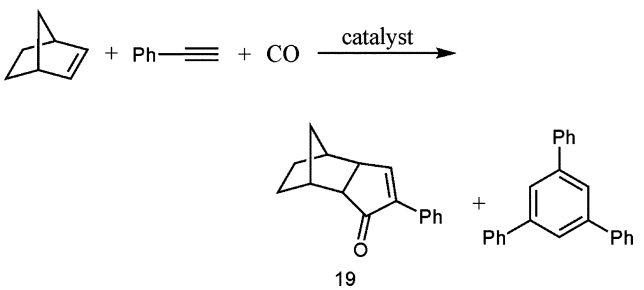

Scheme 2 The cyclisation reaction of norbornene, phenyl acetylene and carbon monoxide in presence of a cobalt carbonyl catalyst to form 4-phenyltricyclo[5.2.1.$0^{2,6}$]dec-4-en-3-one (**19**) and 1,3,5-triphenylbenzene.

The cyclotrimerization of alkynes is a common side reaction that is observed for the Pauson–Khand reaction, and triphenylbenzene is the side-product formed from trimerization of phenyl acetylene. Interestingly, no detectable amount of triphenylbenzene was observed when **16** and **17** were used as catalyst precursors. Even though the cluster most likely acts as a catalyst precursor, the chiral diphosphine ligand may be present in the active catalyst, and the steric bulk of the diphosphine may thus prevent the formation of the sterically demanding by-product triphenylbenzene.

Intramolecular Pauson–Khand reaction. To test for stereoselectivity in intramolecular Pauson–Khand reactions, catalysis of the cyclisation of diethyl allyl propargyl malonate (**20**) (Scheme 3)

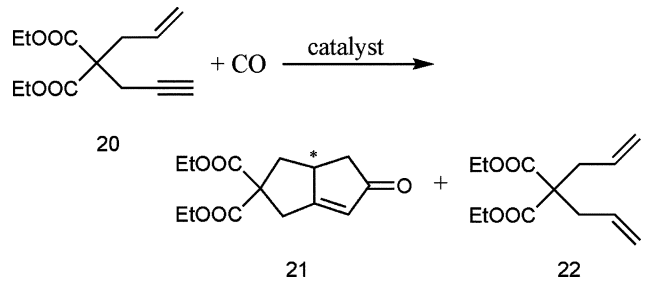

Scheme 3 The cyclisation reaction of diethyl allyl propargyl malonate (**20**) and carbon monoxide in presence of a cobalt catalyst, leading to the formation of 7,7-bis(ethoxycarbonyl)bicycle[3.3.0]-1-octene-3-one (**21**) and diethyl 2,2-diallylmalonate (**22**).

using the chiral methylidyne tricobalt carbonyl clusters **4**, **7**, **12**–**18** were performed at 120 °C in toluene under 10 bar of carbon monoxide for 10 h. As in the intermolecular reaction (*vide supra*), no additives were used.

Similarly to the intermolecular cyclization experiments, there is no evidence that the clusters act as catalysts, but rather as catalyst precursors for the intramolecular cyclisation. Evidence for cluster fragmentation and/or colloidal particle formation was observed, such as a substantial colour change of the reaction solution during the catalytic experiment, deposition of black metallic residues, and no recovery of the original cluster.

The results of the catalytic intramolecular cyclisation reactions are summarised in Table 3. The yield of the desired cyclopentenone varies significantly between the different tests, ranging from very low (**14**, 6%) to relatively good (**7**, 76%). The enantiomeric excess (ee) of 7,7-bis(ethoxycarbonyl)bicycle[3.3.0]-1-octene-3-one (**22**) (Scheme 3) was determined by HPLC analysis using a Chiralpak AD-H analytical column. The enantiomeric excesses obtained, if any, differ notably for the various cluster catalysts, but are consistently low. The general trend in the catalysis experiments is that the clusters that gave (relatively) high product yields generated a racemate, while low conversion of the starting material gave "higher" enantioselectivity. Thus, clusters **7**, **12**, **13** and **18** gave yields of racemic cyclopentenone in the range of 31–76%. The cobalt clusters **14**, **15**, **16** and **17** exhibit the lowest conversions (slowest catalytic rates) but are able to generate enantioselectivity in the intramolecular cyclisation reaction. Cluster **14** that gave the most poor product yield is the one that gives the highest enantioselectivity (13% ee). Clusters **15**, **16** and **17** gave slightly higher yields but very low enantioselectivities. In contrast, high enantioselectivies have been reported for intramolecular Pauson–Khand reactions catalyzed by $Co_2(CO)_8$ with addition of a chiral auxiliary ligand. Cyclisation of **20** catalyzed by $Co_2(CO)_8$/MeO-BIPHEP[33] resulted in 91.5% ee and in a similar reaction using $Co_2(CO)_8$/BINAP[11] 91% ee was obtained.

Table 3 Results from catalytic intramolecular Pauson–Khand synthesis

Entry	Catalyst[a]	Yield[b] (%)	ee (%)[c]
1	**7**	76[d]	Racemate
2	**4**	66[e]	Racemate
3	**12**	54	Racemate
4	**18**	39	Racemate
5	**13**	31	Racemate
6	**16**	27	2 (+)
7	**17**	17	7 (−)
8	**15**	16	7 (−)
9	**14**	6	13 (+)

[a] *Reaction conditions*: *n*(substrate)/*n*(catalyst) = 50, *p*(CO) = 10 bar, *T* = 120 °C, solvent = toluene, duration = 10 h. [b] Isolated yield after prep. TLC (hexane–ethyl acetate 3 : 2 v/v). [c] In cases where ee was obtained, + indicates an excess of first product eluted and − indicates that the second product was in excess. [d] Diethyl 2,2-diallylmalonate (**22**) was isolated (9%). [e] Diethyl 2,2-diallylmalonate (**22**) was isolated (16%).

Conclusions

We have shown that clusters of the general formulae $[Co_3(\mu_3\text{-}CR)_{9-x}(PR'_3)_x]$ (PR'_3 = achiral or chiral monodentate phosphine) and $[Co_3(\mu_3\text{-}CR)_{10}(P\text{–}P)]$ (P–P = chiral diphosphine; two structural isomers) are capable of acting as catalysts/catalyst precursors for both inter- and intramolecular Pauson–Khand reactions with moderate to good yields of cyclopentenones. However, although the intramolecular cyclization reactions catalysed by $[Co_3(\mu_3\text{-}CH)(CO)_7(P\text{–}P)$ (P–P = CHIRAPHOS, NORPHOS, Me-DUPHOS, PROPHOS) demonstrate the feasibility of using such chiral clusters in Pauson–Khand reactions, the enantioselectivities are too poor to make these specific clusters viable catalysts/catalyst precursors for this type of asymmetric reaction.

Experimental

General experimental procedures

The parent clusters $[Co_3(\mu_3\text{-}CH)(CO)_9]$, $[Co_3(\mu_3\text{-}CCO_2Et)(CO)_9]$ and $[Co_3(\mu_3\text{-}CCH_3)(CO)_9]$ were prepared by a literature method.[34] The synthesis of diethyl allyl propargyl malonate (**20**) was also carried out by a literature method.[35] All reactions were performed under an inert atmosphere of either argon or nitrogen, and manipulations of the products were carried out in air. ^1H and ^{31}P NMR spectra were recorded on Varian Unity 300 MHz or Varian Inova 500 MHz spectrometers at 298 K in $CDCl_3$, unless stated otherwise. The ^1H NMR spectra were referenced to solvent signals ($CHCl_3$ = δ7.25) while the ^{31}P NMR spectra were referenced to external 85% H_3PO_4. Infrared spectra were recorded on a Nicolet Avatar 360 FT-IR spectrometer. Thin-layer chromatography was performed on commercially available 20 × 20 cm glass plates, covered with Merck Kieselgel 60 to 0.25 mm or 0.5 mm thickness. In the catalysis experiments, a Parr autoclave fitted with a PTFE liner (30 mL) was used as reaction vessel. Solvents used in synthesis and catalysis experiments were distilled over appropriate drying agents and were deoxygenated by bubbling with nitrogen gas prior to use.

Syntheses

$[Co_3(\mu_3\text{-}CCO_2Et)(CO)_8(PEt_3)]$ (1) and $[Co_3(\mu_3\text{-}CCO_2Et)(CO)_7(PEt_3)_2]$ (3). A total of 100 mg (0.194 mmol) $[Co_3(\mu_3\text{-}CCO_2Et)(CO)_9]$ and 23 mg (0.194 mmol) triethylphosphine were dissolved in 15 mL of dichloromethane and stirred at room temperature for 18 h. The solvent was removed under reduced pressure, the solid obtained was dissolved in a small quantity of dichloromethane, and the products were separated using preparative TLC (eluent: dichloromethane–hexane 3 : 2 v/v). Except for unconsumed starting materials, two products were removed from the TLC plates, extracted with dichloromethane

and dried under vacuum. The first band gave a yellow–orange solid identified as $[Co_3(\mu_3\text{-}CCO_2Et)(CO)_8(PEt_3)]$ (**1**) (47 mg, 40%). (Anal. Calc. for $C_{18}H_{20}O_{10}PCo_3$: C, 35.79 H, 3.34. Found: C, 35.93; H, 3.38%); IR cyclohexane, ν_{CO}/cm^{-1}: 2083 s, 2056 s, 2040 vs, 2029 vs, 2018 s, 1994 w; ^1H NMR: δ 4.28 (q, $J = 14.1$, 7.2 Hz, 2H), 1.79 (dq, $J = 15.9$, 7.8 Hz, 6H) 1.31 (t, $J = 7.2$, 3H), 1.20 (dt, $J = 7.2$, 3.6 Hz, 9H); $^{31}P\{^1H\}$ NMR: δ 39.95 (br s); m/z (FAB): 604 (M^+), and peaks for $[M - nCO]^+$ (n = 1–8), and the second band afforded a yellow solid identified as $[Co_3(\mu_3\text{-}CCO_2Et)(CO)_7(PEt_3)_2]$ (**3**) (15 mg, 11%) (Anal. Calc. for $C_{23}H_{35}O_9P_2Co_3$: C, 39.79; H, 5.08; P, 11. 85. Found: C, 40.33; H, 5.38%); IR cyclohexane, ν_{CO}/cm^{-1}: 2054 s, 2004 vs, 1998 vs, 1981 s, 1963 m, 1854 w, 1825 w; ^1H NMR: δ 4.19 (q, $J = 14.4$, 7.2 Hz, 2H), 1.78 (dq, $J = 15.3$, 7.5 Hz, 12H), 1.28 (t, $J = 7.2$ Hz, 3H), 1.10 (dt, $J = 15.3$, 7.5 Hz, 18H); $^{31}P\{^1H\}$ NMR: δ 52.3 (s); m/z (FAB): 694 (M^+–1) and peaks for $[M - nCO]^+$ (n = 1–7).

$[Co_3(\mu_3\text{-}CH)(CO)_8(PMe_2Ph)]$ (2) and $[Co_3(\mu_3\text{-}CH)\text{-}(CO)_7(PMe_2Ph)_2]$ (4). To a dichloromethane (15 ml) solution of $[Co_3(\mu_3\text{-}CH)(CO)_9]$ (100 mg, 0.226 mmol), PMe_2Ph (31 mg, 0.226 mmol) was added and the reaction mixture was stirred at room temperature for 3 h. The solvent was removed by vacuum and the solid residue was dissolved in a small quantity of dichloromethane and purified by preparative TLC. Elution with hexane–CH_2Cl_2 (4 : 1 v/v) gave three bands, where the first band was unconsumed parent cluster. The second band gave a brown–black solid identified as $[Co_3(\mu_3\text{-}CH)(CO)_8(PMe_2Ph)]$ (**2**) (57 mg, 46%) (Anal. Calc. for $C_{17}H_{12}O_8PCo_3$: C, 36.99; H, 2.19. Found: C, 36.84; H, 2.21%); IR cyclohexane, ν_{CO}/cm^{-1}: 2080 s, 2033 vs, 2025 vs, 2012 s, 1983 w, 1972 w, 1877 w, 1860 w; (solid state): 2074 s, 2033 m, 2019 s, 2004 vs, 1976 w, 1965 s; ^1H NMR: δ 11.01 (s, 1H), 7.36 (m, 2H), 7.23 (s, 3H), 1.21 (d, 3H); (at 203 K): δ 10.60 (br s, 1H), 7.09 (m, 5H), 2.03 (s, 6H); $^{31}P\{^1H\}$ NMR: δ 16.14 (s, br) and (at 203 K) 18.70 (s); m/z (FAB): 552 (M^+) and peaks for $[M - nCO]^+$ (n = 1–8). The third band afforded a yellow–brown solid identified as $[Co_3(\mu_3\text{-}CH)(CO)_7(PMe_2Ph)_2]$ (**4**) (25 mg, 17%) (Anal. Calc. for $C_{24}H_{23}O_7P_2Co_3$: C, 43.53; H, 3.50. Found: C, 43.63; H, 3.41%); IR cyclohexane, ν_{CO}/cm^{-1}: 2046 s, 1994 vs, 1988 sh, 1851 m, 1824 m; ^1H NMR: δ 11.03 (s), 7.75 (m, 4H), 7.52 (m, 6H), 1.75 (d, 12H); $^{31}P\{^1H\}$ NMR: δ 34.28 (s); m/z (FAB): 662 (M^+) and peaks for $[M - nCO]^+$ (n = 1–7). Single crystals of $[Co_3(\mu_3\text{-}CH)(CO)_8(PMe_2Ph)]$ (**2**) suitable for X-ray structure analysis were grown by slow evaporation at −20 °C from a hexane–dichloromethane mixture.

$[Co_3(\mu_3\text{-}CCO_2Et)(CO)_6(PEt_3)_3]$ (5). To a solution of $[Co_3(\mu_3\text{-}CCO_2Et)(CO)_9]$ (100 mg, 0.194 mmol) in 15 mL of dichloromethane, an excess of triethylphosphine (71 mg, 0.6 mmol) was added. The reaction mixture was stirred at room temperature for 18 h. The solvent was removed under reduced pressure, the solid obtained was dissolved in a small quantity of dichloromethane and the products were separated using preparative TLC (eluent: dichloromethane–hexane 3 : 2 v/v). Except for unconsumed starting materials, one product was removed from the TLC plates and extracted with dichloromethane and dried under vacuum. The orange solid obtained was identified as $[Co_3(\mu_3\text{-}CCO_2Et)(CO)_6\{PEt_3\}_3]$ (**5**) (76 mg, 50%) (Anal. Calc. for $C_{28}H_{50}O_8P_3Co_3$: C, 42.87; H, 6.42; P, 11. 85. Found: C, 43.85; H, 6.48; P, 11.47%); IR cyclohexane, ν_{CO}/cm^{-1}: 2002 m, 1979 vs, 1966 s, 1946 w, 1814 s, 1803 w; ^1H NMR: δ 3.73 (m, 2H), 1.70 (t, $J = 7.6$ Hz, 18H), 1.33 (m, 3H), 1.01 (m, 27H); $^{31}P\{^1H\}$ NMR: δ 30.74 (s). MS (FAB$^+$, m/z): 784 (M^+) and peaks for $[M - nCO]^+$ (n = 1–6).

$[Co_3(\mu_3\text{-}CH)(CO)_6(PMe_2Ph)_3]$ (6). To a dichloromethane (15 ml) solution of $[Co_3(\mu_3\text{-}CH)(CO)_9]$ (70 mg, 0.158 mmol), PMe_2Ph (90 mg, 0.652 mmol) was added and the reaction mixture was stirred at room temperature for 2 h. The solvent was removed under vacuum. The compound was purified by recrystallization at −20 °C in hexane and afforded orange crystals identified as $[Co_3(\mu_3\text{-}CH)(CO)_6(PMe_2Ph)_3]$ (**6**) (92 mg, 75%) (Anal. Calc. for $C_{31}H_{34}O_6P_3Co_3$: C, 48.21; H, 4.44, P, 12.03. Found: C, 48.02; H, 4.56, P, 11.53%); IR cyclohexane, ν_{CO}/cm^{-1}: 2002 s, 1968 vs, 1808 vs; ^1H NMR: δ 10.67 (s, 1H), 7.72 (m, 6H), 7.47 (m, 9H), 1.71 (d, 18H); $^{31}P\{^1H\}$ NMR: δ 14.99 (s); m/z (FAB): 772 (M^+) and peaks for $[M - nCO]^+$ (n = 1–6).

$[Co_3(\mu_3\text{-}CH)(CO)_8\{(S)\text{-NMDPP}\}]$ (7). To a toluene solution (10 mL) of $[Co_3(\mu_3\text{-}CH)(CO)_9]$ (100 mg, 0.226 mmol), (*S*)-NMDPP [= ((1*S*)-2-isopropyl-5-methylcyclohexyl)diphenylphosphine] (73 mg, 0.226 mmol) was added and the reaction was stirred at 90 °C for 4 h. The solvent was removed under vacuum and the residue was purified using preparative TLC. Besides a stationary band (decomposed product(s)), elution with hexane–dichloromethane (9 : 1 v/v) gave three bands. The three products were removed from the TLC plates, extracted with dichloromethane and dried under vacuum. The first product was unconsumed $[Co_3(\mu_3\text{-}CH)(CO)_9]$ (15 mg). The second product was only obtained in trace amounts and has not been characterized. The third product was identified as $[Co_3(\mu_3\text{-}CH)(CO)_7\{(S)\text{-NMDPP}\}]$ (**7**) (85 mg, 51%), (Anal. Calc. for $C_{31}H_{30}O_8PCo_3$: C, 50.43; H, 4.10. Found: C, 51.03; H, 4.23%); IR cyclohexane, ν_{CO}/cm^{-1}: 2078 s, 2041 vs, 2015 vs, 1980 sh, 1952 w, 1858 m; ^1H NMR: δ 11.02 (s, 1H), 7.50 (m, 10H), 3.07 (t, $J = 15.0$ Hz, 1H), 2.15 (m, 2H), 1.75 (m, 4H), 1.60 (m, 1H), 1.22 (d, $J = 15.0$ Hz, 1H), 0.90 (q, $J = 12.0$, 6.0 Hz, 9H), 0.27 (d, $J = 6.0$ Hz, 1H); $^{31}P\{^1H\}$ NMR: δ 60.0 (s); m/z (FAB): 738 (M^+) and peaks for $[M - nCO]^+$ (n = 1–8).

$[\{Co_3(\mu_3\text{-}CH)(CO)_8\}_2(\mu\text{-dppe})]$ (8) and $[Co_3(\mu_3\text{-}CH)(CO)_7(\mu\text{-dppe})]$ (10). To a toluene (15 ml) solution of 100 mg (0.226 mmol) $[Co_3(\mu_3\text{-}CH)(CO)_9]$, 90 mg (0.226 mmol) of dppe [= 1,2-bis(diphenylphosphino)ethane] was added and the reaction mixture was stirred at room temperature for 3 h. The solvent was removed under vacuum and the solid residue was purified using preparative TLC. Elution with a mixture of hexane–dichloromethane (7 : 3 v/v) gave three bands, where the band with highest R_f was identified as the unconsumed parent tricobalt alkylidyne cluster. The second band gave $[\{Co_3(\mu_3\text{-}CH)(CO)_8\}_2(\mu\text{-dppe})]$ (**8**) (69 mg, 25%). Anal. Calc. for $C_{44}H_{26}O_{16}P_2Co_6$: C, 43.10; H, 2.14. Found: C, 43.07; H, 2.15%); IR cyclohexane, ν_{CO}/cm^{-1}: 2080 s, 2037 s, 2024 vs, 2014 m, 1991 w, 1970 w, 1880 m; ^1H NMR: δ 7.33 (m, 20H), 2.19 (br s, 4H); $^{31}P\{^1H\}$ NMR: δ 46.02 (s); m/z (FAB): 1226 (M^+) and peaks for $[M - nCO]^+$ (n = 1–16). The third band afforded $[Co_3(\mu_3\text{-}CH)(CO)_7(\mu\text{-dppe})]$ (**10**) (90 mg, 51%) (Anal. Calc. for $C_{34}H_{25}O_7P_2Co_3$: C, 52.07; H, 3.21. Found: C, 51.79; H, 3.34%); IR cyclohexane, ν_{CO}/cm^{-1}: 2051 vs, 2024 vs, 2000 s, 1981 m, 1973 w, 1941 m; ^1H NMR: δ 7.46 (m, 20H), 2.11 (m, 4H); $^{31}P\{^1H\}$ NMR: δ 53.57 (s); m/z (FAB): 784 (M^+) and peaks for $[M - nCO]^+$ (n = 1–7).

[{$Co_3(\mu_3$-CH)$(CO)_8\}_2(\mu$-dppm)] (9) and [$Co_3(\mu_3$-CH)$(CO)_7(\mu$-dppm)] (11). To a toluene (15 ml) solution of [$Co_3(\mu_3$-CH)$(CO)_9$] (100 mg, 0.226 mmol), dppm (87 mg, 0.226 mmol) was added and the reaction mixture was stirred at room temperature for 3 h. The solvent was evaporated under vacuum and the solid residue was dissolved in a small quantity of dichloromethane and purified on preparative TLC plates. Two products, one yellow and the other dark brown, were isolated from the TLC plates, extracted with dichloromethane and dried under vacuum. The yellow solid was identified as [{$Co_3(\mu_3$-CH)$(CO)_8\}_2(\mu$-dppm)] (**9**) (15 mg, 4%), (Anal. Calc. for $C_{43}H_{24}O_{16}P_2Co_6$: C, 42.61; H, 2.00. Found: C, 43.17; H, 2.19%); IR cyclohexane, ν_{CO}/cm^{-1}: 2075 s, 2036 s, 2008 vs, 1992 m, 1972 w; ^{1}H NMR: δ 7.25–7.43 (m, 20H), 2.86 (m, 2H); ^{31}P{^{1}H} NMR: insufficient sample. Mass spectrum (*m*/*z*): 1212 (M^+) and peaks for [M − *n*CO]$^+$ (*n* = 1–6). The dark brown product was identified as [$Co_3(\mu_3$-CH)$(CO)_7(\mu$-dppm)] (**11**) (117 mg, 67%), (Anal. Calc. for $C_{33}H_{23}O_7P_2Co_3$: C, 51.46; H, 3.01. Found: C, 51.34; H, 3.10%); IR cyclohexane, ν_{CO}/cm^{-1}: 2061 s, 2008 vs, 1992 w, 1970 w, 1958 vw; ^{1}H NMR: δ 12.10 (s, 1H), 7.74–7.14 (m, 20H), 4.04 (q, *J* = 20.0, 12.0 Hz, 1H), 3.40 (q, *J* = 24.0, 12.0 Hz, 1H); ^{31}P{^{1}H} NMR: δ 42.22 (s). *m*/*z* (FAB): 770 (M^+) and peaks for [M − *n*CO]$^+$ (*n* = 1–7). An alternative synthetic procedure for the preparation of **11** has been published by M. I. Bruce *et al.*[13]

[$Co_3(\mu_3$-CH)$(CO)_7\{\mu$-1,2-(*R*,*R*)-DIPAMP}] (12). To a toluene solution (10 mL) of [$Co_3(\mu_3$-CH)$(CO)_9$] (30 mg, 67 μmol), DIPAMP [= (1*R*,2*R*)-bis(2-methoxyphenylphenylphosphino)ethane] (31 mg, 67 μmol) was added and the reaction mixture was stirred at room temperature for 2.5 h. The solvent was removed under vacuum and the black solid residue was purified by preparative TLC. Besides a stationary brown band (decomposed material(s)), elution with hexane-dichloromethane (3 : 2 v/v) gave a single band, which was removed from the TLC plates and extracted with dichloromethane. The solvent was removed under vacuum, resulting in a black solid identified as [$Co_3(\mu_3$-CH)$(CO)_7\{$(*R*,*R*)-DIPAMP}] (**12**) (40 mg, 70%), (Anal. Calc. for $C_{36}H_{29}O_9P_2Co_3$: C, 51.21; H, 3.46. Found: C, 51.11; H, 3.59%); IR hexane, ν_{CO}/cm^{-1}: 2055 s, 2001 vs, 1992 sh, 1985 w, 1969 m; ^{1}H NMR: δ 7.38 (m, 10H), 6.93 (m, 8H), 3.86 (br, 3H), 3.41 (s br, 3H), 2.39 (br, 2H), 2.16 (br, 2H); ^{31}P{^{1}H} NMR: δ 51.3 (s); *m*/*z* (FAB): 844 (M^+) and peaks for [M − *n*CO]$^+$ (*n* = 1–7). Single crystals suitable for X-ray analysis were grown by slow evaporation from a hexane-dichloromethane mixture at room temperature.

[$Co_3(\mu_3$-CH)$(CO)_7\{$(*R*)-BINAP}] (13). In a two-necked round bottom flask fitted with a condenser [$Co_3(\mu_3$-CH)$(CO)_9$] (25 mg, 57 μmol) and (*R*)-BINAP [= (*R*)-(+)-2,2′-bis(diphenylphosphino)-1,1′-binapthyl] (35 mg, 56 μmol) were dissolved in CH_2Cl_2 (12 ml), heated gently and maintained at reflux for 22 h. During the course of reaction, the solution changed colour from deep purple to black–brown. The solvent was removed using rotary evaporation. The black–brown solid obtained was dissolved in approx. 2 ml of CH_2Cl_2 and purified using preparative TLC (Merck Kieselgel 60, 0.5 mm thickness; eluent: hexane–CH_2Cl_2 3 : 1 v/v). Except for a brown stationary band (probably decomposed material) and traces of unconsumed [$Co_3(\mu$-CH)$(CO)_9$], three bands were eluted. The green–black main product was scraped of the TLC plate and dissolved in CH_2Cl_2. The silica was filtered off and the product solution was concentrated and dried under vacuum. A green black solid was obtained and identified as [$Co_3(\mu_3$-CH)$(CO)_7\{$(*R*)-BINAP}] (29 mg, 51%) (**13**); IR hexane, ν_{CO}/cm^{-1}: 2058 vs, 2010 s, 2005 vs, 1990 vw, 1973 w, 1966 w, 1950 vw, 1755 m, 1750 m; ^{1}H NMR: δ 12.45 (s, 1H), 8.79–6.11 (m, 32H); ^{31}P{^{1}H} NMR: 59.8 (s), 46.2 (s); *m*/*z* (FAB): 983 (M^+ − CO) and peaks for [M − *n*CO]$^+$ (*n* = 2–7).

[$Co_3(\mu_3$-CH)$(CO)_7\{$(*S*,*S*)-CHIRAPHOS}] (14). A hexane solution (5 ml) of [$Co_3(\mu_3$-CH)$(CO)_9$] (10 mg, 22.6 μmol) and (*S*,*S*)-CHIRAPHOS [= (2*S*,3*S*)-(−)-bis(diphenylphosphino)butane] (10 mg, 23.5 μmol) was heated slowly to reflux under vigorous stirring. The reaction was monitored by spot TLC (eluent: hexane–CH_2Cl_2 2 : 1 v/v). When all starting cluster was consumed, the reaction mixture was transferred to a Pasteur pipette prepared with glass wool and a few centimetres of silica on top. Traces of the parent cluster were eluted with pure hexane and then the green product was eluted using hexane–CH_2Cl_2 (2 : 1 v/v). The isolated green product was concentrated and dried under vacuum, yielding a dark green product, [$Co_3(\mu_3$-CH)$(CO)_7$(*S*,*S*)-CHIRAPHOS] (**14**) (18 mg, 98%), IR hexane, ν_{CO}/cm^{-1}: 2059 vs, 2016 vs, 2002 vs, 1986 m, 1973 w, 1946 vw; ^{1}H NMR: δ10.86 (s, 1H), 7.78–7.12 (m, 20H), 2.30 (s, 2H), 0.82 (s, 6H); ^{31}P{H} NMR: 77.5 (s); *m*/*z* (FAB): 812 (M^+) and peaks for [M − *n*CO]$^+$ (*n* = 1–7).

[$Co_3(\mu_3$-CH)$(CO)_7\{$(*R*,*R*)-NORPHOS}] (15). [$Co_3(\mu_3$-CH)$(CO)_9$] (10 mg, 23 μmol) and (*R*,*R*)-NORPHOS [= (2R,3R)-(−)-2,3-bis(diphenylphosphino)bicyclo[2.2.1]hept-5-ene] (11 mg, 24 μmol) were dissolved in hexane (10 mL). The reaction mixture was heated gently to 40 °C. The reaction was monitored by spot TLC (hexane–dichloromethane 1 : 1 v/v) and after 40 min, when all ligand was consumed, the solvent was evaporated under reduced pressure. The resultant green black-residue was dissolved in a small quantity of dichloromethane and purified using a short column packed with silica 60 (5 mm × 50 mm). The column was eluted with hexane to remove unconsumed starting material leaving a green–black solid, which eluted with a mixture of hexane–dichloromethane (1 : 1 v/v). The green-black fraction was collected and concentrated using rotary evaporation to afford a green–black solid identified as [$Co_3(\mu_3$-CH)$(CO)_7\{$(*R*,*R*)-NORPHOS}] (**15**) (11 mg, 55%). IR hexane, ν_{CO}/cm^{-1}: 2058 vs, 2013 s, 2003 vs, 1990 w, 1970 w, 1936 vw; ^{1}H NMR: δ 10.91 (s, 1H), 8.07 7.11 (m, 20H), 5.96 (s, 1H), 4.15 (s, 1H), 3.06–1.33 (m, 6H); ^{31}P{^{1}H} NMR: δ 60.8 (s), 51.3 (s); *m*/*z* (FAB): 821 (M^+–CO) and peaks for [M − *n*CO]$^+$ (*n* = 2–7).

[$Co_3(\mu_3$-CH)$(CO)_7\{$(*R*)-PROPHOS}] (16). In a two-neck round-bottom flask fitted with a condenser, [$Co_3(\mu_3$-CH)$(CO)_9$] (10 mg, 23 μmol) and (*R*)-PROPHOS [= (*R*)-(+)-1,2-bis(diphenylphosphino)propane] (9 mg, 22 μmol) were dissolved in hexane (12 ml) and stirred at room temperature (~23 °C) for 10 min. The reaction mixture was then heated at 40 °C, whereupon the colour of the solution gradually changed from deep purple to black–brown. After 1 h the solvent was removed using rotary evaporation. The black–brown solid obtained was purified using a short column packed with silica Kieselgel 60 (5 mm × 50 mm). The column was eluted with hexane to remove any unconsumed starting material, leaving a dark green solid which was eluted with a mixture of hexane–CH_2Cl_2 (1 : 1 v/v). The green fraction was collected and concentrated using rotary

evaporation, yielding a green–black solid identified as $[Co_3(\mu_3\text{-}CH)(CO)_7\{(R)\text{-PROPHOS}\}]$ (**16**) (10.4 mg, 59%) (Anal. Calc. for $C_{35}H_{27}O_7P_2Co_3$: C, 52.66; H, 3.41. Found: C, 52.04; H, 3.67%); IR hexane, ν_{CO}/cm^{-1}: 2059 s, 2011 s, 2003 vs, 1991 w, 1971 m; ^1H NMR: δ 7.73–6.81 (m, 20H), 2.34 (s, 3H), 2.09 (m, 2H), 1.67 (m, 1H), 1.26 (s, 3H), 0.96 (m, 2H), 0.85 (m, 1H); $^{31}P\{^1H\}$ NMR: δ 62.76 (s), 53.41 (s); *m/z* (FAB): 798 (M^+) and peaks for $[M - n CO]^+$ ($n = 1$–7).

$[Co_3(\mu_3\text{-}CH)(CO)_7\{(R,R)\text{-Me-DUPHOS}\}]$ (17). To a hexane solution (8 ml) of $[Co_3(\mu_3\text{-}CH)(CO)_9]$ (40 mg, 91 μmol) was added (*R*,*R*)-Me-DUPHOS [= (−)-1,2-bis((2*R*,5*R*)-2,5-dimethylphospholano)benzene] (27 mg, 88 μmol) and the reaction mixture was heated slowly to 40 °C under vigorous stirring. After 30 min the reaction mixture was transferred to a Pasteur pipette, prepared with glass wool and a few centimetres of silica on top. Traces of the parent cluster were eluted with pure hexane and then an orange compound was eluted using hexane–CH_2Cl_2 (1 : 1 v/v). The isolated orange product was concentrated and dried under vacuum, yielding a bright red product, $[Co_3(\mu_3\text{-}CH)(CO)_7\{(R,R)\text{-Me-DUPHOS}\}]$ (**17**) (43 mg, 70%). IR hexane, ν_{CO}/cm^{-1}: 2056 s, 2024 s, 1994 s, 1883 vs, 1863 m, 1819 m; ^1H NMR: δ 7.83–7.52 (m, 4H), 6.35 (s, 1H), 2.90 (s, 2H), 2.37 (m, 4H), 2.15 (m, 2H), 1.8–1.38 (m, 4H), 1.14 (dd, 1H, $J = 6.7$ Hz, $J = 19.0$ Hz), 0.65 (dd, 1H, $J = 6.5$ Hz, $J = 14.1$ Hz); $^{31}P\{^1H\}$ NMR: δ 93.7; *m/z* (FAB): 692 (M^+) and peaks for $[M - n CO]^+$ ($n = 1$–7). Single crystals suitable for crystallographic X-ray structure determination were grown by slow evaporation at room temperature from a mixture of hexane and CH_2Cl_2.

$[Co_3(\mu_3\text{-}CH)(CO)_7\{(R)\text{-}(S)\text{-Josiphos3}\}]$ (18). In a 25-ml two-necked round-bottom flask fitted with a condenser and a dropping funnel, $[Co_3(\mu_3\text{-}CH)(CO)_9]$ (16 mg, 36 μmol) was dissolved in CH_2Cl_2 (5 ml) and heated to reflux. The dropping funnel was charged with (*R*)-(*S*)-Josiphos3 [= (*R*)-(−)-1-[(*S*)-2-(dicyclohexylphosphino)ferrocenyl]ethyldicyclohexylphosphine] (20 mg, 33 μmol) dissolved in CH_2Cl_2 (5 ml) and the solution was added dropwise to the refluxing cluster solution. After 5 min., the solution turned deep red–black and spot TLC (eluent: hexane–CH_2Cl_2 1 : 1 v/v) showed one new orange–red product. The solvent was evaporated and the resultant solid residue was dissolved in a minimum amount of dichloromethane and purified through a short plug of silica, eluting initially with hexane, followed by hexane–dichloromethane 1 : 1 (v/v), and finally CH_2Cl_2. One red fraction was collected and concentrated under vacuum. The red solid residue obtained was identified as $[Co_3(\mu_3\text{-}CH)(CO)_7\{(R)\text{-}(S)\text{-Josiphos3}\}]$ (**18**) (27 mg, 83%). IR hexane, ν_{CO}/cm^{-1}: 2050 s, 2018 vs, 1998 m, 1989 vs, 1982 m, 1956 m, 1924 w, 1879 w, 1854 m, 1818 m, 1755 m; ^1H NMR: δ 9.75 (s, 0.32 H), 4.25 (m, 8H), 2.79–0.91 (m, 44H); $^{31}P\{^1H\}$ NMR: δ 32.7 (s), 37.2 (s) 39.9 (s), 54.2 (s), 61.2 (s), 69.8 (s); *m/z* (FAB) 993 ($M^+ + 1$) and peaks for $[M - n CO]^+$ ($n = 1$–7).

Catalysis experiments

Intermolecular Pauson–Khand reactions. In a typical experiment, the autoclave was loaded with catalyst (14 mg) and the substrates norbornene and phenyl acetylene, each in a 50 molar excess relative to the catalyst. Toluene (5 mL) was added and the autoclave was purged several times before being pressurized with 10 bar of CO. The reaction was continuously stirred with a magnetic stirrer and heated at 120 °C for 10 h. The reaction vessel was allowed to cool down to room temperature before it was carefully opened. The reaction mixture was transferred to a round-bottom flask and the solvent was removed under vacuum. The oily residue was purified using preparative TLC, eluting with a hexane-ethyl acetate mixture (4:1 v/v). Except for starting materials, two products were removed from the TLC plates, extracted with dichloromethane and dried under vacuum. The first product was a white solid identified as 1,3,5-triphenylbenzene and the second product was identified as 4-phenyltricyclo[5.2.1.$0^{2,6}$]dec-4-en-3-one (**19**), ^1H NMR: δ 7.68 (d, $J = 7.5$ Hz, 2H), 7.63 (d, $J = 3.0$ Hz, 1H), 7.36 (t, $J = 7.5$ Hz, 2H), 7.31 (d, $J = 7.5$ Hz, 1H), 2.69 (t, $J = 3.75$ Hz, 1H), 2.49 (d, $J = 4.0$ Hz, 1H), 2.36 (d, $J = 5.0$ Hz, 1H), 2.27 (d, $J = 4.5$ Hz, 1H), 1.69 (m, 1H), 1.61 (m, 1H), 1.33 (m, 2H), 1.11 (d, $J = 10.5$ Hz, 1H), 1.0 (d, $J = 10.5$ Hz, 1H).

Intramolecular Pauson–Khand reaction. In a typical experiment, the autoclave was loaded with catalyst (14 mg) and diethyl allyl propargyl malonate (**20**), in a 50-fold molar excess. Toluene (5 mL) was added and the autoclave was purged several times before being pressurized with 10 bar of CO. The reaction was continuously stirred with a magnetic stirrer and heated at 120 °C for 10 h. The reaction vessel was allowed to cool down to room temperature before carefully opened. The reaction mixture was transferred to a round-bottomed flask and the solvent was removed under vacuum. The oily residue was purified on preparative TLC, eluting with a hexane–ethyl acetate mixture (3 : 2 v/v). Except for starting material, two products were removed from the TLC plates, extracted with dichloromethane and dried under vacuum. The two transparent oils obtained were identified as 7,7-bis(ethoxycarbonyl)bicyclo[3.3.0]-1-octene-3-one (**21**), ^1H NMR: δ 5.91 (s, 1H), 4.21 (dq, $J = 14.0$, 7.0 Hz, 4H), 3.33 (d, $J = 19.0$ Hz, 1H), 3.23 (d, $J = 19.0$ Hz, 1H), 3.09 (ddd, $J = 2.5$, 3.5, 5.0 Hz, 1H), 2.78 (dd, $J = 7.5$, 13.0 Hz, 1H), 2.62 (dd, $J = 6.5$, 18.0 Hz, 1H), 2.13 (dd, $J = 3.0$, 17.5 Hz, 1H), 1.71 (t, $J = 13.0$ Hz, 1H), 1.25 (dt, $J = 7.0$, 14.0 Hz, 6H), and diethyl 2,2-diallylmalonate (**22**), ^1H NMR: δ 5.64 (m, 2H), 5.09 (dd, $J = 8.0$, 2.0 Hz, 4H), 4.17 (q, $J = 7.0$ Hz, 4H), 2.62 (d, $J = 7.5$ Hz, 4H), 1.23 (t, $J = 7.0$ Hz, 6H).

HPLC analysis. The enantiomeric excess of the product, 7,7-bis(ethoxycarbonyl)bicyclo[3.3.0]-1-octene-3-one (**21**), obtained in catalytic experiments was assessed by HPLC analysis using a Varian Prostar chromatograph (PDA detector) with a Chiralpak AD-H analytical column. The eluent was *n*-hexane–isopropanol (9 : 1 v/v) and the flow rate was 0.5 mL min^{-1}. The retention times for the first and second enantiomers were 16.9 and 17.8 min, respectively.

X-Ray crystallography

The diffraction data were collected at 293 K for clusters **2** and **6** using a Bruker SMART APEX diffractometer. The Bruker SMART and SAINT programs[36] were used for cell refinement and data reduction. The structure solutions were carried out using SHELXS 97,[37] and SHELXL[38] was used for structure refinements.

Diffraction data were collected at 294 K for clusters **12** and **17** on a Nonius CAD-4 diffractometer. CAD4 v 5.0[39] were used

Table 4 Crystallographic data for $[Co_3(\mu_3\text{-}CH)(CO)_8(PMe_2Ph)]$ (**2**), $[Co_3(\mu_3\text{-}CH)(CO)_6(PMe_2Ph)_3]$ (**6**), $[Co_3(\mu_3\text{-}CH)(CO)_7(\mu\text{-}1,2\text{-DIPAMP})]$ (**12**) and $[Co_3(\mu_3\text{-}CH)(CO)_7(1,1\text{-DUPHOS})]$ (**17**)

	2	**6**	**12**	**17**
Empirical formula	$C_{17}H_{12}Co_3O_8P$	$C_{31}H_{34}Co_3O_6P_3$	$C_{36}H_{29}Co_3P_2O_9$	$C_{26}H_{29}Co_3O_7P_2$
M_r	552.03	772.28	844.4	692.3
T/K	293(2)	293(2)	294	294
λ/Å	0.71073	0.71073	0.71073	0.71073
Crystal system	Monoclinic	Triclinic	Orthorhombic	Orthorhombic
Space group	$P2_1$	$P1$	$P2_12_12_1$	$P2_12_12_1$
a/Å	8.7435(7)	10.1219(18)	11.968(2)	9.803(1)
b/Å	14.8061(12)	10.4665(19)	12.618(2)	16.155(2)
c/Å	9.0608(8)	10.5068(19)	24.770(5)	18.477(2)
V/Å^3	1053.31(15)	859.3(3)	3741(1)	2926.2(6)
Z	2	1	4	4
D_c/g/cm^3	1.741	1.492	1.50	1.57
μ/mm^{-1}	2.450	1.610	1.450	1.829
Crystal size/mm	0.40 × 0.20 × 0.15	0.37 × 0.25 × 0.06	0.36 × 0.24 × 0.17	0.25 × 0.18 × 0.12
h range	−7 to 11	−13 to 13	0 to 14	0 to 11
k range	−19 to 18	−13 to 13	0 to 15	0 to 19
l range	−12 to 8	−13 to 13	0 to 29	0 to 22
Reflections collected	6738	7355	3673	2908
Independent reflections	4622	6667	3673	2907
Data/restraints/parameters	4622/1/262	6667/3/394	2687/0/324	2520/0/343
Goodness-of-fit on F^2	0.872	0.985	1.24	1.09
$R1$	0.0272	0.0440	0.05	0.028
$wR2$	0.0696[a]	0.0802[a]	0.066[b]	0.033[b]
Weighting scheme	$x = 0.0531$, $y = 0.0000$	$x = 0.0150$, $y = 0.0000$	$x = 0.0004$	$x = 0.0004$
$\Delta\rho_{max/min}$/e Å^{-3}	0.345/−0.189	0.538/−0.357	1.18/−0.69	0.34/−035
Abs. struct. parameter	0.282(13)	0.015(15)	0.00(4)	0.00(2)

[a] $w = 1/[\sigma^2(F_o^2) + (xP)^2 + yP]$, $P = (F_o^2 + 2F_c^2)/3$. [b] $w = 1/[\sigma^2(F_o^2) + xF^2]$.

for cell refinement and data reduction. The structure solution was carried out using SIR92[40] and RAELS[41] was used for structure refinements. The absolute structures for clusters **2**, **6**, **12** and **17** were determined on the basis of the Flack index[42] during the refinement process.

Relevant crystal, data collection and refinement data for the X-ray crystal structures of $Co_3(\mu_3\text{-}CH)(CO)_8(PMe_2Ph)]$ (**2**), $[Co_3(\mu_3\text{-}CH)(CO)_6(PMe_2Ph)_3]$ (**6**), $[Co_3(\mu_3\text{-}CH)(CO)_7(\mu\text{-}1,2\text{-DIPAMP})]$ (**12**) and $[Co_3(\mu_3\text{-}CH)(CO)_7(1,1\text{-DUPHOS})]$ (**17**) are summarised in Table 4.

CCDC reference numbers 668301–668304.

For crystallographic data in CIF or other electronic format see DOI: 10.1039/b717698h

Acknowledgements

This research has been sponsored by The Royal Swedish Academy of Sciences, the Crafoord Foundation and the Swedish Research Council (VR). A. J. Deeming thanks the Wenner-Gren Foundation for a visiting professorship at Lund University. V. Moberg thanks the Solander program for a travel award that enabled him to carry out research at the University of New South Wales. We thank Cecilia Olsson for helpful assistance with the HPLC analysis of the potentially enantioselective Pauson–Khand reactions.

References

1 I. U. Khand, G. R. Knox, P. L. Pauson and W. E. Watts, *J. Chem. Soc. D*, 1971, 36.
2 T. Sugihara, M. Yamaguchi and M. Nishizawa, *Chem.–Eur. J.*, 2001, **7**, 1589.
3 N. E. Schore and M. C. Crondacy, *J. Org. Chem.*, 1981, **46**, 5436–5438.
4 (*a*) S. Shambayati, W. E. Crowe and S. L. Schreiber, *Tetrahedron Lett.*, 1990, **31**, 5289; (*b*) N. Jeong, Y. K. Chung, B. Y. Lee, S. H. Lee and S.-E. Yoo, *Synlett*, 1991, 204.
5 (*a*) R. J. Dennenberg and D. J. Darensbourg, *Inorg. Chem.*, 1972, **11**, 72; (*b*) J. D. Atwood and T. L. Brown, *J. Am. Chem. Soc.*, 1976, **98**, 3160; (*c*) D. J. Darensbourg and R. L. Kump, *Inorg. Chem.*, 1978, **17**, 2680.
6 R. B. Grossman and S. L. Buchwald, *J. Org. Chem.*, 1992, **57**, 5803.
7 B. M. Trost and A. B. Pinkerton, *Org. Lett.*, 2000, **11**, 1603.
8 I. U. Khand, G. R. Knox, P. L. Pauson, W. E. Watts and M. I. Foreman, *J. Chem. Soc., Perkin Trans. 1*, 1973, 977.
9 T. Sugihara and M. Yamaguchi, *J. Am. Chem. Soc.*, 1998, **120**, 10782.
10 P. J. Dyson, *Chem. Rev.*, 2004, **248**, 2443.
11 K. Hiroi, T. Watanabe, R. Kawagishi and I. Abe, *Tetrahedron: Asymmetry*, 2000, **11**, 797.
12 (*a*) X. Verdaguer, A. Moyano, M. A. Pericas, A. Riera, V. Bernardes, A. E. Greene, A. Alvarez-Larena and J. F. Piniella, *J. Am. Chem. Soc.*, 1994, **116**, 2153–2154; (*b*) X. Verdaguer, J. Vazquez, G. Fuster, V. Bernardes-Genisson, A. E. Greene, A. Moyano, M. A. Pericas and A. Riera, *J. Org. Chem.*, 1998, **63**, 7037–7052; (*c*) D. Konya, F. Robert, Y. Gimbert and A. E. Greene, *Tetrahedron Lett.*, 2004, **45**, 6975–6978.
13 M. I. Bruce, K. A. Kramarczuk, G. J. Perkins, B. W. Skelton, A. H. White and N. N. Zaitseva, *J. Cluster Sci.*, 2004, **15**, 119.
14 G. A. Acum, M. J. Mays, P. R. Raithby and G. A. Solan, *J. Organomet. Chem.*, 1996, **508**, 137.
15 W. H. Watson, S. G. Bodige, K. Ejsmont, J. Liu and M. G. Richmond, *J. Organomet. Chem.*, 2006, **691**, 3609, and references therein.
16 V. Moberg, R. Duquesne and E. Nordlander, unpublished results.
17 S. P. Tunik, I. O. Koshevoy, A. J. Poe, D. H. Farrar, E. Nordlander, T. A. Pakkanen and M. Haukka, *Dalton Trans.*, 2003, 2457.
18 P. W. Sutton and L. F. Dahl, *J. Am. Chem. Soc.*, 1967, **89**, 261.
19 M. Ahlgrén, T. T. Pakkanen and I. Tahvanainen, *J. Organomet. Chem.*, 1987, **323**, 91.

20 D. C. Miller, R. C. Gearhart and T. B. Brill, *J. Organomet. Chem.*, 1979, **169**, 395.
21 J. D. King, M. Monari and E. Nordlander, *J. Organomet. Chem.*, 1999, **573**, 272.
22 S. J. Maginn, *Acta Crystallogr., Sect. C*, 1990, **46**, 2339.
23 M. D. Brice, B. R. Penfold, W. T. Robinson and S. R. Tylor, *Inorg. Chem.*, 1970, **9**, 362.
24 W. H. Watson, S. G. Bodige, K. Ejsmont, J. Liu and M. G. Richmond, *J. Organomet. Chem.*, 2006, **691**, 3609.
25 L. Pauling, *Proc. Natl. Acad. Sci. USA*, 1976, **73**, 4290.
26 (*a*) R. G. Cunningham, L. R. Hanton, S. D. Jensen, B. H. Robinson and J. Simpson, *Organometallics*, 1987, **6**, 1470; (*b*) R. P. Aggarwal, N. G. Connelly, M. C. Crespo, B. J. Dunne, P. M. Hopkins and A. G. Orpen, *J. Chem. Soc., Dalton Trans.*, 1992, 655.
27 S. G. Bott, H. Shen and M. G. Richmond, *Struct. Chem.*, 2001, **12**, 225.
28 G. R. Desiraju, *J. Chem. Soc., Dalton Trans.*, 2000, 3745.
29 (*a*) D. Braga, F. Grepioni, K. Biradha, V. R. Pedireddi and G. R. Desiraju, *J. Am. Chem. Soc.*, 1995, **117**, 3156; (*b*) D. Braga and F. Grepioni, *Acc. Chem. Res.*, 1997, **30**, 81.
30 A. J. Downard, B. H. Robinson and J. Simpson, *Organometallics*, 1986, **5**, 1122.
31 V. Moberg, P. Homanen, S. Selva, R. Persson, M. Haukka, T. A. Pakkanen, M. Monari and E. Nordlander, *Dalton Trans.*, 2006, 279.
32 P. Homanen, R. Persson, M. Haukka, T. A. Pakkanen and E. Nordlander, *Organometallics*, 2000, **19**, 5568.
33 T. M. Schmid and G. Consiglio, *Tetrahedron: Asymmetry*, 2004, **15**, 2205.
34 D. Seyferth, J. E. Hallgren and P. L. K. Hung, *J. Organomet. Chem.*, 1973, **50**, 265.
35 (*a*) K. D. Dötz and M. Popall, *Tetrahedron*, 1985, **41**, 5797; (*b*) A. K. Pearson and R. A. Dubbert, *Organometallics*, 1994, **13**, 1656.
36 *SMART and SAINT Software Reference Manuals*, Version 5.051 (Windows NT Version), Bruker Analytical X-ray Instruments Inc., Madison, WI, 1998.
37 G. M. Sheldrick, *SHELXS97, Program for Crystal Structure Determination*, University of Göttingen, Germany, 1997.
38 G. M. Sheldrick, *SHELXL97, Program for Crystal Structure Refinement*, University of Göttingen, Germany, 1997.
39 J. D. Schagen, L. Strayer, F. van Meurs and G. Williams, *CAD4 Operator's Guide*, Delft Instruments, Delft, Netherlands, 1989.
40 A. Altomare, M. C. Burla, G. Camalli, G. Cascarano, C. Giacovazzo, A. Gualiardi and G. Polidori, *J. Appl. Crystallogr.*, 1994, **27**, 435.
41 A. D. Rae, *RAELS96: A Comprehensive Constrained Least-Square Refinement Program*, Australian National University, Canberra, A. C. T., Australia, 1996.
42 H. D. Flack, *Acta Crystallogr., Sect. A*, 1983, **39**, 876.